MAPPING OF CONTACT RESISTANCE AND LOCATING SHUNTS ON SOLAR CELLS USING RESISTANCE ANALYSIS BY MAPPING OF POTENTIAL (RAMP) TECHNIQUES

A.S.H. van der Heide, A. Schönecker, G.P. Wyers, W.C. Sinke
ECN Solar Energy
P.O. Box 1, 1755 ZG Petten, The Netherlands
Phone: +31 224 564176 Fax: +31 224 563214
E-mail: vanderheide@ecn.nl

ABSTRACT: Two new techniques are described, one to locate shunts on solar cells (PRAMP) and one to map the specific contact resistance ρ_c of the front side metallisation (SCRAMP). In addition, the influence of a varying ρ_c on the diode factor n and the series resistance of a cell was calculated. The new techniques are both based on the mapping of a current induced potential to analyse the resistance problems. The PRAMP scan proved to be an easy technique to detect shunts with a resolution of ~1 mm; disadvantage is the impossibility to detect shunts below metal, advantage is the simple equipment that is needed. More important is the SCRAMP scan that can map ρ_c on a 10 x 10 cm^2 cell in 20 min. Compared to the standard techniques, the advantages of SCRAMP are its speed and the fact that it does not rely on the assumption that ρ_c is the same for all fingers. The SCRAMP scans showed that screen printed silicon solar cells with low fill factor have large lateral ρ_c variations. A computer program was written to calculate the influence of these large ρ_c variations on the I-V curve of a cell. It was found that the diode factor of the cell increases due to ρ_c variations (even values above 2 can be reached), while the series resistance value does not increase significantly.
Keywords: Contact Resistance – 1: Diode Factor – 2: Shunts - 3

1. INTRODUCTION

To optimise solar cell efficiency, resistance losses have to be minimised. The purpose of this work is to describe techniques that are suitable to map the specific contact resistance ρ_c and to locate shunts. As they are both based on mapping of the (current induced) potential on a solar cell, they are grouped under the general name "Resistance Analysis by Mapping of Potential" (RAMP).

In addition, it was investigated by calculations how lateral ρ_c variations influence the I-V curve of a solar cell. This was done because large ρ_c variations that were found on the solar cells were suspected to increase the diode factor n or simulate a second diode current increase (depending on the fit model used).

2. THE RAMP TECHNIQUES

The RAMP techniques (patent pending for both [1]) measure the potential between the back of the solar cell and a probe that scans the top surface. To let the probe penetrate the isolating anti-reflection coating, it is made of tungsten and scratches the surface during the scan. The difference between the two RAMP techniques is the way in which current is generated.

2.1 The Parallel RAMP (PRAMP) technique

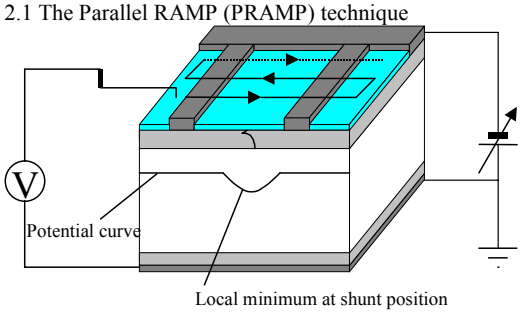

Fig. 1: Schematic drawing of the PRAMP technique.

The PRAMP technique, used to locate shunts, is shown schematically in Fig. 1. The scan is performed in the dark; the current is generated by applying a forward bias voltage across the cell that is low enough for a negligible current flow through a cell without shunts (≈ 0.3 V for a silicon cell).

Under these conditions, current can only flow through the cell at places where shunts are present. Because the emitter has a relatively high resistance, a potential gradient will exist across the emitter in the direction of a shunt location, with the shunt located at the local potential minimum. A shunt below the metallisation cannot be detected, because of the high conductivity of the metal. An example of a shunt scan parallel to the busbars is shown in Fig. 2.

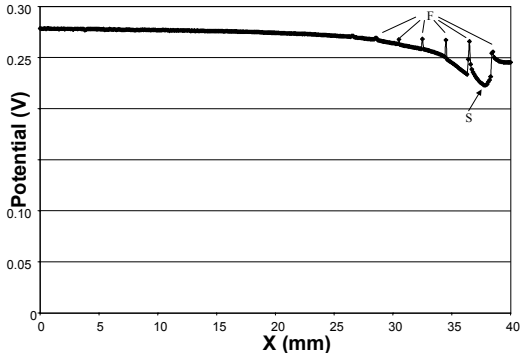

Fig. 2: PRAMP scan, showing a shunt (S) near the edge of the cell; the fingers (F) are also indicated.

In Fig. 3, a 2D picture of a PRAMP scan is shown.

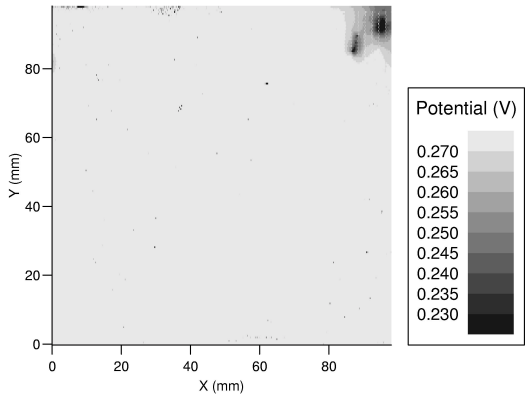

Fig. 3: 2D PRAMP scan on a 10 x 10 cm² cell; a shunt is present in the upper right corner of the cell. After removal of that corner, the parallel resistance of the cell increased from 5 to 30 Ω.

The time needed to make a PRAMP scan on a 10 x 10 cm² wafer is 40 min and the resolution is ~1 mm. The main advantage of the technique compared to other shunt locating techniques, such as thermography [2], is the simple equipment that is needed.

2.2 The Specific Contact RAMP (SCRAMP) technique

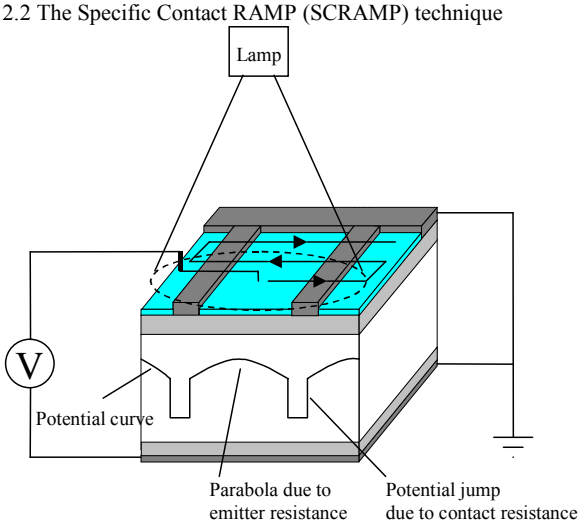

Fig. 4: Schematic drawing of the SCRAMP technique.

The SCRAMP technique is displayed in Fig. 4. For this technique, where ρ_c is mapped, the cell is short-circuited and current is generated by a light beam larger than the finger separation that is centered around the probe. Short circuiting the cell causes the generated current to be nearly constant over the whole cell and also minimises possible shunt currents. The current has to be transported away from the point of generation, causing potential gradients over the surface of the solar cell. The ρ_c is proportional to the potential jump V_c at the finger; the sheet resistance to the curvature of the parabola between the fingers. An example of a SCRAMP line scan is displayed in Fig. 5.

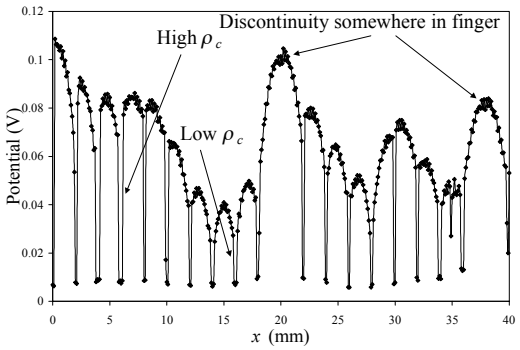

Fig. 5: Example of a SCRAMP line scan.

Compared to traditional techniques [3], the main advantages of SCRAMP are the speed (20 min for a 10 x 10 cm² cell), the relatively simple equipment and the fact that it does not rely on the assumption that ρ_c is the same for all fingers.

2.3 Calculation of ρ_c from a SCRAMP scan

The potential curve between the fingers for an illuminated, short circuited cell will be calculated first.
Let the current to a finger, per unit length of finger, be denoted by i. The gradient of i equals the light generated current density J_L :

$$\frac{di}{dx} = J_L \qquad (1)$$

It can be assumed that the current flows horizontally to a finger, through the emitter. Using this assumption, i can be expressed in terms of the emitter sheet resistance ρ_s and the gradient of the potential dV/dx:

$$i = -\frac{1}{\rho_s}\frac{dV}{dx} \qquad (2)$$

It is assumed that ρ_s is constant between the fingers. Substituting (2) in (1) gives the following differential equation for the potential between the fingers:

$$\frac{d^2V}{dx^2} = -\rho_s J_L \qquad (3)$$

which has the equation of a parabola as solution:

$$V(x) = -\tfrac{1}{2}\rho_s J_L x^2 + C_1 x + C_2 \qquad (4)$$

where C_1, C_2 are constants determined by the ρ_c values and the potentials at the bordering fingers; J_L is determined experimentally and is assumed to be constant over the whole cell. ρ_s is calculated from the curvature of the parabola:

$$\rho_s = -\frac{1}{J_L}\frac{d^2V}{dx^2} \qquad (5)$$

To calculate ρ_c, the following relation is used:

$$\rho_c = \frac{V_c}{J_c} = \frac{w_{eff}V_c}{i_c} \qquad (6)$$

where J_c is the current density through the finger-silicon contact, i_c the current entering the finger per unit length and w_{eff} the effective width of the finger, which can be smaller than the real finger width w. This is the case when ρ_c is low and the sheet resistance below the finger $\rho_{s,bf}$ is

high, because the current then 'wants' to enter the finger as soon as possible instead of continuing through the high resistance emitter. The result: most of the current flows at the finger edges and nothing at the finger centre. In a quantitative way, this effect is described by the current transfer length L_T, which can be seen as the distance a lateral current will penetrate below the finger, and is given by:

$$L_T = \sqrt{\frac{\rho_c}{\rho_{s,bf}}} \qquad (7)$$

It can be derived [4] that w_{eff} can be expressed in terms of L_T as follows: $w_{eff} = 2L_T/\coth(w/2L_T)$. Substituting w_{eff} in (6) gives:

$$\rho_c = \frac{2L_T V_c}{i_c \coth(w/2L_T)} \qquad (8)$$

The value of i_c can be deduced from ρ_s and the potential gradients at both sides of the finger, using (2).
The expression for ρ_c then finally becomes:

$$\rho_c = \frac{2L_T V_c}{\left(\frac{1}{\rho_{s,L}}\left|\frac{dV_L}{dx}\right| + \frac{1}{\rho_{s,R}}\left|\frac{dV_R}{dx}\right|\right)\coth(w/2L_T)} \qquad (9)$$

where the indices L and R are used to indicate at the left side and at the right side of the finger, respectively. Absolute values of the derivatives are taken because only the magnitude of the current is of importance, not the direction. Equation (9) can be simplified in two steps.

The first approximation is to assume that $w_{eff}=w$; this removes the necessity to know $\rho_{s,bf}$ (cannot be determined from the SCRAMP scan) and leads to an upper bound $\rho_{c,max}$ which converges to the correct value for large ρ_c:

$$\rho_{c,\max} = \frac{wV_c}{i_c} \qquad (10)$$

It was calculated that for $w<L_T$, the deviation of $\rho_{c,max}$ from the real ρ_c will be smaller than 10%. Using typical values for screen printed solar cells, this means ρ_c should be >20-30 mΩcm^2. The second step is to introduce the approximation $i_c = dJ_L$, with d the distance between the fingers, that can be used as long as neighbouring fingers do not differ too much in ρ_c (so they receive the same current). Substitution for i_c in (10) then gives the following good approximation:

$$\rho_{c,\max} = \frac{w}{dJ_L} V_c \qquad (11)$$

It is convenient for scan interpretation to adjust the light intensity so that $J_L=w/d$, because $\rho_{c,max}$ will then be equal to the measured V_c.

2.4 Results of 2D SCRAMP scans

Two examples of 2D SCRAMP scans will be discussed. The first scan was performed to check the quality of the firing of a screen printed metallisation through a TiO_2 anti-reflection coating. The result is shown in Fig. 5:

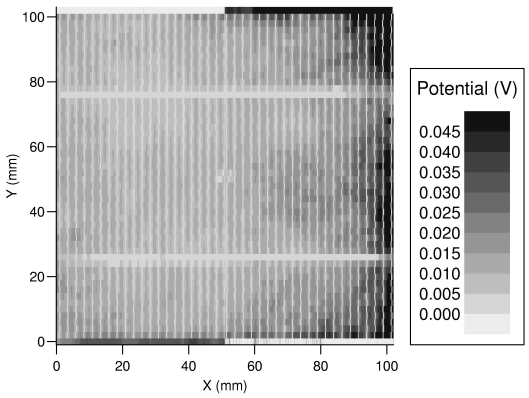

Fig. 5: Result of a SCRAMP scan on a cell with a TiO_2 anti-reflection coating on it. Note that ρ_c is higher on the right side of the wafer.

Interestingly, the part of the cell having higher ρ_c values corresponded to the region having a different coating-colour, indicating a different coating thickness. It must be noted that a correlation between coating colour and ρ_c was specific for this particular case. In most cases measured so far, ρ_c variations were found which were not correlated to coating colour differences.

The second SCRAMP scan, on a cell where firing through a silicon nitride coating was performed, is shown in Fig. 6. It is clear that large ρ_c variations are present on this cell, which increases the diode factor as will be shown in the next section.

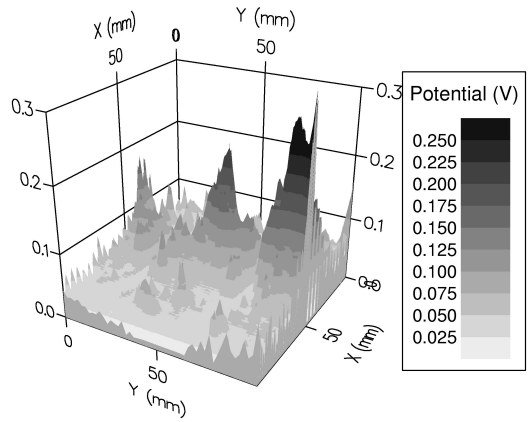

Fig. 6: Three dimensional graph of a SCRAMP scan on a 10 x 10 cm^2 cell. Large variations in ρ_c are present on this cell, for which FF = 71.8% and n = 1.84. J_L was chosen to be 50 mA/cm^2 (which is w/d) so that the potential jump in V equals ρ_c in Ωcm^2.

The reason for the measured ρ_c variations was not further examined. In general, there are many possibilities, such as inhomogeneous firing temperatures in belt furnaces, incomplete removal of phosphorous glass after emitter diffusion, varying anti-reflection coating thickness or locally varying screen printing quality.

In a production line, the real cause of the problem can easily be analysed by setting up an experiment where wafers undergo different process steps with varying

orientation. The SCRAMP scans of the cells can then be used to determine the critical process step(s).

3. INFLUENCE OF ρ_C VARIATIONS ON THE I-V CURVE OF A SOLAR CELL

In the following analysis, only the one-diode model was used to model the I-V curve. The fit algorithm is described in [5]. It should be noted that an increase of the diode factor used in the one-diode model will be reflected in an increase of the second diode current when the two-diode model is used.

The calculation of the influence of ρ_c variations on the I-V curve was based on a distributed diode model, in which the current density is not constant, but is voltage- and position-dependent. The following differential equation, which can be obtained from equation (3) by adding a diode term to J_L on the right side of the equation, has to be solved between the fingers:

$$\frac{d^2V}{dx^2} = -\rho_s \left[J_L - J_0 (e^{\frac{qV(x)}{nkT}} - 1) \right] \quad (12)$$

where J_0 is the saturation current density, q the elementary charge, n the diode factor, k the Boltzmann constant and T the absolute temperature. The equation can only be solved numerically, with boundary conditions that are determined by the contact resistances and the potentials at the fingers.

When the potential function between the fingers has been calculated, the total generated current between the fingers can be found. This current is proportional to the sum of the derivatives of the potential at the fingers (was also used for ρ_c calculation). By calculating the generated current for different finger potentials, an I-V curve can be calculated for the area between the fingers for given ρ_c and ρ_s.

By combining I-V curves for different values of ρ_c, the influence of lateral ρ_c variations on a solar cell I-V curve can be calculated. As a test, I-V curves having a diode factor of 1.3 were calculated for ρ_c = 10 mΩcm^2 and for ρ_c = 150 mΩcm^2. Then the combined I-V curve was found by averaging the current of both curves at each potential. All three curves were fitted by the one diode model. The calculated curves are shown in Fig. 7, together with their fit parameters. The symbol r_{series} designates a measure for the series resistance of the cell.

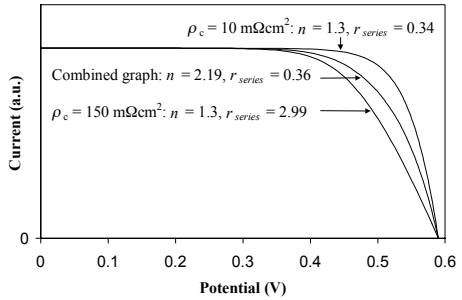

Fig. 7: Calculated I-V curves with fit parameters for ρ_c = 10 mΩcm^2, ρ_c = 150 mΩcm^2 and the combined graph. The combined graph has a much higher n value, while the series resistance is only slightly increased.

It was found that the diode factors and series resistances of the individual curves were determined correctly, while the combined curve has an increased diode factor of 2.19 and a series resistance value which is only slightly increased. This finding contradicts the general idea that all series resistance effects can be found back in the series resistance of the entire cell.

Two examples of experiments that illustrate the effect on the diode factor found by the calculations will be discussed. Firstly, removing that half of a solar cell having a high ρ_c resulted in a decrease of the diode factor (2.05 to 1.68). Secondly, the diode factor of a particular cell decreased from 2.24 to 1.63 for a decrease in light intensity from 1 sun to 0.2 sun. This is to be expected if the high diode factor is a resistance effect (and is not expected if it is due to recombination), since the currents will be lower at low light intensity. Consequently, the performance of a high diode factor cell on a yearly basis will be better than expected, since the mean light intensity will be lower than 1 sun.

4. CONCLUSIONS

It can be concluded that powerful techniques have been developed to locate shunts (PRAMP) and to map ρ_c (SCRAMP). These techniques can be applied as tools to analyse problems in processing of screen printed solar cells.

The main advantage of the PRAMP technique is the simple equipment needed; shunts below metallisation cannot be detected, and the resolution is ~1 mm.

The SCRAMP technique is much faster (20 min for 10 x 10 cm^2 cell) than existing techniques for measuring ρ_c and is not based on the assumption that all fingers have the same ρ_c.

It appeared that on screen printed solar cells, large ρ_c variations can be found. Therefore, it was calculated what the influence of these variations on the I-V curve of a cell would be. It was found that the diode factor is strongly increased by large ρ_c variations, while there is little influence on the series resistance of the cell.

ACKNOWLEDGEMENTS

This work was funded by ECN's long term energy research programme ENGINE.

REFERENCES

[1] Dutch patent application 1013204, October 1999.
[2] O. Breitenstein, M. Langenkamp, Proc. 2nd World Conference on Photovoltaic Solar Energy Conversion (1998) 1382.
[3] G.K. Reeves, H.B. Harrison, IEEE Electron Device Letters **3** (1982) 111.
[4] H.H. Berger, Journal of the Electrochemical Society **119** (1972) 507.
[5] A.R. Burgers, J.A. Eikelboom, A. Schönecker, W.C. Sinke, Proc. 25th IEEE Photovoltaic Specialists Conference (1996) 569.